



Published in final edited form as:

J Immunol. 2013 February 15; 190(4): 1447–1456. doi:10.4049/jimmunol.1202115.

TLR9 Promotes Tolerance by Restricting Survival of Anergic Anti-DNA B Cells Yet is Also Required for Their Activation¹

Kevin M. Nickerson^{*}, Sean R. Christensen^{*}, Jaime L. Cullen^{*}, Wenzhao Meng[†], Eline T. Luning Prak[†], and Mark J. Shlomchik^{*}

^{*}Departments of Laboratory Medicine and Immunobiology, Yale University School of Medicine, New Haven, CT 06510

[†]Department of Pathology and Laboratory Medicine, Perelman School of Medicine, University of Pennsylvania, Philadelphia, PA 19104

Abstract

Nucleic acid reactive B cells frequently arise in the bone marrow but are tolerized by mechanisms including receptor editing, functional anergy, and/or deletion. TLR9, a sensor of endosomal dsDNA, both promotes and regulates systemic autoimmunity *in vivo*, but the precise nature of its apparently contradictory roles in autoimmunity remained unclear. Here, using the 3H9 anti-DNA BCR transgene in the autoimmune-prone MRL.*Fas^{lpr}* mouse model of systemic lupus erythematosus, we identify the stages at which TLR9 contributes to establishing and breaking B cell tolerance. Although TLR9 is dispensable for light chain editing during B cell development in the bone marrow, TLR9 limits anti-DNA B cell lifespan in the periphery and is thus tolerogenic. In the absence of TLR9, anti-DNA B cells have much longer lifespans and accumulate in the follicle, neither activated nor deleted. These cells retain some characteristics of anergic cells, in that they have elevated basal BCR signaling but impaired induced responses and downregulate their cell surface BCR expression. In contrast, while TLR9-intact anergic B cells accumulate near the T/B border, TLR9-deficient anti-DNA B cells are somewhat more dispersed throughout the follicle. Nonetheless, in older autoimmune-prone animals, TLR9 expression specifically within the B cell compartment is required for spontaneous peripheral activation of anti-DNA B cells and their differentiation into AFCs via an extrafollicular pathway. Thus, TLR9 has paradoxical roles in regulating anti-DNA B cells: it helps purge the peripheral repertoire of autoreactive cells yet is also required for their activation.

Introduction

Autoreactive B cell receptors (BCRs) arise as a result of V(D)J recombination. As many as 55-75% of developing B cells display BCRs with measurable affinity for self epitopes (1). Several self-tolerance mechanisms efficiently eliminate the majority of self-reactive BCR specificities prior to or shortly after entry into the mature B cell repertoire. These include editing of autoreactive BCRs through additional rounds of recombination at the light (L) chain loci, deletion of autoreactive B cells, or the acquisition of a functionally unresponsive phenotype termed anergy (2, 3).

¹This work was supported by the National Institutes of Health Grant P01-AR050256. K.M.N. was supported by the National Research Service Award training grant 5T32-HL007974 and a grant from the S.L.E. Lupus Foundation. E.L.P. and W.M. were supported by the Lupus Research Institute and the Arthritis Foundation. The authors have no conflicting financial interests.

Corresponding Author: Dr. Mark Shlomchik Department of Laboratory Medicine Yale University School of Medicine P.O. Box 208035 New Haven, CT 06520 ph: (203) 737-2089 fax: (203) 785-5415 mark.shlomchik@yale.edu.

Recently, we and others have shown that Toll-like receptor 9 (TLR9), an endosomal innate immune sensor of dsDNA (4), is required for formation of spontaneous anti-DNA autoAbs in several *in vivo* mouse models of systemic lupus erythematosus (SLE) (5-10). These findings are consistent with a model in which autoreactive B cells in SLE break tolerance due to the unique ability of nucleic-acid containing self Ags to co-engage the BCR and one or more innate immune sensors of nucleic acids, including TLR7 or TLR9, even in the absence of specific T cell help (11). *In vitro* evidence supports a role for TLR9 in this context (12). However, *in vivo* the precise roles of TLR9 in autoimmunity may be more complex. Additional signals from both T cells and myeloid cells might substitute for TLR9 in B cells. Moreover, because TLR9 expression begins early in B cell development (13), TLR9 could play roles in B cell repertoire selection and the establishment of central tolerance, as has been suggested recently (14). To address the B cell-specific roles of TLR9 throughout autoreactive B cell development and activation, we examined the effect of TLR9 deficiency in the 3H9 anti-DNA BCR model (15, 16).

3H9 is an anti-DNA mAb, the H chain of which confers affinity for DNA via arginine residues in its CDRs (17). Depending on the Ig L chain with which the 3H9 V_H pairs, the resulting Ab or BCR can bind to ssDNA or dsDNA (18). A subset of L chains (termed editors) significantly reduce the H chain's affinity for DNA (19). When the 3H9 V_H is expressed as a transgene (Tg) in the BALB/c strain, developing anti-dsDNA B cells are deleted, receptor-edited or anergized so that the peripheral B cell repertoire is enriched for editor L chains, and anti-dsDNA Abs are not detectable in the serum (15, 20-22). In contrast, when the Tg is expressed on the autoimmune-predisposed genetic background MRL.*Fas*^{lpr}, a subpopulation of autoreactive cells at any given time have escaped tolerance and differentiate into short-lived plasmablasts that secrete anti-DNA autoAbs (16).

To investigate the role of TLR9 in establishing and breaking tolerance in autoimmune MRL.*Fas*^{lpr} mice, we studied mixed bone marrow (BM) chimeras lacking TLR9 in B cells and crossed the 3H9 anti-DNA Tg onto the *Tlr9*^{-/-} MRL.*Fas*^{lpr} genetic background. Here we show that the absence of TLR9 expression in B cells prevents the spontaneous production of anti-DNA autoAbs via an extrafollicular (EF) pathway. Surprisingly, we found that TLR9 was not just required for activation, but also controlled self-tolerance. DNA-reactive 3H9/Vλ1 B cells in TLR9-deficient MRL.*Fas*^{lpr} mice were neither activated nor deleted. Rather, they entered the B cell follicle and accumulated as long-lived resting cells despite evidence of Ag exposure and anergy. These results identify a novel protective role for TLR9 in regulating autoreactive B cell lifespan and localization.

Materials and Methods

Mice

Mixed BM chimeras were prepared by whole-body x-irradiation of *JH*^{-/-} MRL.*Fas*^{lpr} recipients with 750-800 rads. After 1-2 hrs, animals were given $\sim 4 \times 10^6$ BM cells from donors mixed at indicated ratios by *i.v.* injection. Mice transgenic for 3H9 IgH have been previously described (15, 16). *Tlr9*^{-/-} mice on the MRL/MpJ-*Fas*^{lpr/lpr} background have been previously described (6). Mice were backcrossed for an additional eight generations to the MRL/MpJ-*Fas*^{lpr/lpr/2J} genetic background (Jackson Labs #006825) before intercross. All animal work was approved by the Yale Institutional Animal Care and Use Committee.

Measurement of serum autoAbs and ELISPOTs

Anti-nucleosome ELISA was performed as described (6). For total IgM ELISA, plates were coated with purified rat anti-mouse IgM (clone B7-6). Specific Ab were detected with alkaline phosphatase-conjugated goat anti-mouse IgM or IgG (Southern Biotech,

Birmingham, AL) and absorbance at 405 nm was compared to an anti-nucleosome 3H9/V κ 1 IgM (23), anti-nucleosome PL2-3 (24), or anti-TNP IgM, κ (Becton Dickinson, Franklin Lakes, NJ) for quantitation. HEp-2 ANA (Antibodies, Inc., Davis, CA) were performed as described (6). Anti- λ 1 ELISPOTs were performed as described (25) except plates were coated with rat anti-mouse IgM (clone B7-6) and detection antibody was biotinylated anti- λ 1 clone R11-153 (Becton Dickinson) followed by SA-AP (Southern Biotech).

Flow cytometry, cell sorting and quantitative PCR

Surface staining was performed in ice-cold PBS containing 3% FCS in the presence of 2.4G2 and ethidium monoazide bromide (EMA). Cells were fixed in PBS + 1% PFA. Flow cytometry was performed on a BD LSRII and analyzed in FlowJo (Tree Star, Ashland, OR). Cell sorting was performed on a BD FACSAria.

Ab clones used for surface or intracellular staining were specific for: CD44 (Pgp1 or 1M7), CD86 (GL1), CD19 (1D3.2), CD22 (Cy34.1), B220/CD45R (RA3-6B2), λ 1 (R11-153), λ x (10C5), CD138 (281-2), CD4 (GK1.5), CD43 (S7), IgMa (RS3.1), CD93 (AA4.1), λ -1/2 (JC5), BrdU (PRB-1) and p-Syk (17A/P-ZAP70).

For BrdU labeling, mice were given an *i.p.* injection of 0.5 mg BrdU in PBS every 12 hrs for 2 or 4 days. To measure BrdU incorporation, cells were stained for surface markers and then resuspended in 0.15 M NaCl solution and fixed by dropwise addition of cold ethanol to a final concentration of 70% ethanol. Cells were further treated with 1% PFA and 0.1% Tween-20 in PBS for 30' at room temperature followed by overnight incubation at 4°C. Fixed cells were treated with 100 Kunitz units of DNase (Sigma-Aldrich) in 0.15 M NaCl + 4.2 mM MgCl₂ for 30' at room temperature before the addition of anti-BrdU-Alexa647 (clone PRB1, Life Technologies, Carlsbad, CA) and SA-APC-Cy7 (Becton Dickinson).

For measurement of phosphorylated Syk, splenocytes were disaggregated directly into RPMI containing 1% PFA and fixed for 15' at room temperature. Following RBC lysis with ACK, splenocytes were washed in ice-cold TBS containing 1% BSA then fixed in cold methanol for 30'. Cells were washed with TBS/BSA and either treated or mock-treated with 50 units calf intestinal alkaline phosphatase (New England Biolabs, Ipswich, MA) at 37°C for 15'. Cells were then washed and costained for surface and intracellular markers.

For measurement of Ca⁺² flux, splenocytes were disaggregated into RPMI + 5% FCS. 1 \times 10⁷ RBC-lysed splenocytes were incubated with 5 μ g/mL Indo1-AM reporter dye (Life Technologies) in 1 mL RPMI at 37°C for 30'. Cells were washed with HBSS and surface stained. Data were collected for 1' to establish a baseline prior to the addition of anti-IgM clone B7-6 to a final concentration 15 μ g/mL, and 5' of additional data were collected.

For qPCR, genomic DNA was isolated from sorted B cells using the Gentra Puregene Tissue Kit (Qiagen, Valencia, CA). qPCR was performed in duplicate as described (26).

Immunofluorescence

7 μ m spleen sections were prepared from OCT-frozen tissues and fixed in cold acetone for 10'. Slides were blocked in PBS with 1% BSA (w/v), 0.1% Tween and 10% normal rat serum for 20'. Slides were stained with anti-CD19-Alexa488 (1D3.2), anti-lambda1-biotin (R11-153), anti-F4/80-Alexa647 and CD4-PacificBlue (GK1.5) in blocking buffer for 1 hr then washed 3x in PBS/BSA/Tween followed by immersion in PBS. Slides were then stained with SA-Alexa555 in blocking buffer. Sections were covered with ProLong Anti-Fade Gold (Life Technologies) and a cover slip.

Microscopy was performed on a Nikon Eclipse Ti-U microscope as tiled multi-field images collected with a Nikon CFI Plan Apo 20× 0.75 NA objective and a Retiga 2000R monochrome camera in NIS-Elements AR software. Images were converted to 8-bit RGB in Adobe Photoshop for analysis.

For analysis of $\lambda 1^+$ cell distribution in the FO, images of individual follicles were cropped in Photoshop and analyzed with CellProfiler ver. 2.0 (r10997) software (27). Briefly, the algorithm identified $\lambda 1^+$ cells and measured their total area within two regions. One region was the portion of the CD19⁺ B cell FO within 50 microns of the CD4⁺ T cell zone: CD19⁺ and CD4⁺ regions were manually drawn on their respective single color images, and the border region was computed by expanding the CD4⁺ region by 50 microns in every direction and masking on the intersection of this expanded mask with the CD19⁺ region. The other region was the whole CD19⁺ FO. The ratio of $\lambda 1^+$ pixels in these two regions, normalized for the relative areas of the regions, was defined as the distribution index. Images in which the area of the T/B border was less than 20% or more than 80% of the area of the B cell FO were considered to be atypical cross-sections and were excluded from analysis.

Statistical analysis

Unless otherwise stated, statistical comparisons were by two-tailed Mann-Whitney. Significance values are: * p<0.05 ; ** p<0.01 ; *** p<0.001 as calculated by GraphPad Prism software.

Results

B cell expression of TLR9 is required for anti-DNA generation in lupus mice

Anti-nucleosome autoAbs were reduced in MRL.*Fas^{lpr}* lupus-prone mice genetically deficient in TLR9 (5). However, these animals had markedly exacerbated disease, suggesting complex roles for TLR9 in both promoting and regulating autoimmunity (5, 6). TLR9 is expressed in B cells from at least the pro-B stage onward (13), but is also expressed in other hematopoietic lineages including macrophages and DCs. To determine whether the requirement for TLR9 in anti-nucleosome Ab production was B cell intrinsic, we prepared mixed BM chimeras in which TLR9 deficiency was restricted primarily to the B cell compartment. In this experimental system (Fig. 1A), B-cell deficient (*J_H^{-/-}*) MRL.*Fas^{lpr}* recipients were irradiated and reconstituted with a mix of 80% *J_H^{-/-} Tlr9^{+/+}* BM and either 20% *J_H^{+/+} Tlr9^{+/+}* (B.9^{+/+} group) or 20% *J_H^{+/+} Tlr9^{-/-}* BM (B.9^{-/-} group). Only *J_H^{+/+}* BM is capable of generating B cells, while cells of other hematopoietic lineages are derived from both donors. Control recipients were provided with BM from only *J_H^{+/+} Tlr9^{+/+}* (All.9^{+/+} group) or only *J_H^{+/+} Tlr9^{-/-}* donors (All.9^{-/-} group). Extent of chimerism was confirmed by quantitative real-time PCR (data not shown).

Restriction of *Tlr9*-deficiency to only the hematopoietic compartment resulted in a shift in the dominant serum ANA pattern from a DNA-associated homogenous nuclear staining pattern (Fig. 1B, All.9^{+/+} group) to a speckled nuclear or cytoplasmic staining pattern (Fig. 1B, All.9^{-/-} group), similar to intact MRL.*Fas^{lpr}* lacking TLR9 in all tissues (5, 6). This shift was also seen when TLR9 was absent specifically in B cells but present in most non-B cells (Fig. 1B, B.9^{+/+} versus B.9^{-/-} groups). Positive mitotic chromatin staining in the ANA (Fig. 1C) and anti-nucleosome IgG autoAbs (Fig. 1D) also required TLR9 expression specifically in the B cell compartment, indicating that B cell intrinsic expression of TLR9 is necessary for anti-nucleosome autoAb in lupus-prone mice.

TLR9 is not required for L chain editing

Since TLR9 is expressed from early in B cell development (13) and components of the TLR9 signaling pathway have been implicated in central tolerance (14), we examined the requirements for TLR9 in L chain editing and development of anti-DNA B cells using the 3H9 Tg MRL.*Fas^{lpr}* system, in which L chain usage is a surrogate marker for autoreactivity amid a restricted but polyclonal repertoire. We sorted developing B cell fractions by FACS from the BM of 6-8 wk old 3H9⁺ MRL.*Fas^{lpr}* mice that were either *Tlr9^{+/+}* or *Tlr9^{-/-}* (Fig. 2A) and measured the relative extent of genomic L chain rearrangement to the kappa recombination sequence (RS), a direct measure of attempted L chain editing (28). We found no difference in V κ -RS rearrangement frequencies between TLR9-deficient or -sufficient 3H9⁺ developing B cell Fractions A-C⁺ that have not begun L chain rearrangement, in Fractions D or E that should be undergoing receptor editing (28), or among mature recirculating B cells (Fr. F) (Fig. 2B).

V λ x is a serologically detectable editor of 3H9 IgH (19) and an increase in the frequency of V λ x-expressing cells would thus directly reflect increased editing activity. Indeed, although there were no differences in the overall sizes of any of the developing compartments between 3H9⁺ *Tlr9^{+/+}* or 3H9⁺ *Tlr9^{-/-}* MRL.*Fas^{lpr}* animals (Supplemental Fig. 1), V λ x-expressing B cells were increased in frequency in Fr. E developing B cells in 3H9⁺ MRL.*Fas^{lpr}* compared to non-Tg animals (Fig. 2D), consistent with the previously described increase in λ x L chain usage by peripheral B cells in the related 3H9/56R BALB/c model (19, 21). However, the frequency of edited λ x⁺ B cells was not different between *Tlr9*-intact or -deficient 3H9⁺ MRL.*Fas^{lpr}* mice in either Fr. E or Fr. F (Fig. 2D), suggesting that TLR9 does not affect receptor editing of anti-DNA B cells during development. TLR9 deficiency also had no impact on the frequency of cells using V λ 1, a light chain that permits dsDNA binding when paired with 3H9 IgH (16, 29), among the developing Fraction E B cells (Fig. 2C). Intriguingly, we observed an increase in the frequency of λ 1⁺ cells among recirculating mature 3H9⁺ Fr. F B cells when TLR9 was absent, as will be further investigated below.

TLR9 is required for anti-nucleosome production in 3H9 Tg MRL.*Fas^{lpr}* mice

Since TLR9 did not affect primary repertoire development in 3H9⁺ mice, we examined whether DNA-reactive B cells were dependent on TLR9 for activation and differentiation into AFC. Sera from 3H9⁺ *Tlr9^{+/+}* MRL.*Fas^{lpr}* or 3H9⁺ *Tlr9^{-/-}* MRL.*Fas^{lpr}* at 13-20 wks of age were assessed for anti-nucleosome Abs by ELISA (Fig. 3A). *Tlr9* was indeed required for production of anti-nucleosome IgM Abs in the 3H9 model; whereas total serum IgM titers were similar in *Tlr9*-intact and *Tlr9*-deficient animals (Fig. 3B).

Cells expressing λ 1 are anergic anti-DNA B cells in 3H9 Tg animals (16, 29). We first asked whether λ 1⁺ anti-DNA B cells could become AFCs in the absence of TLR9. λ 1⁺ IgM ELISPOT-forming cells, which were present at high frequency in 3H9 *Tlr9^{+/+}* MRL.*Fas^{lpr}* spleens, were undetectable in the spleens of 3H9⁺ *Tlr9^{-/-}* MRL.*Fas^{lpr}* mice (Fig. 3C). Similarly, λ 1⁺ cells with an AFC phenotype were not observed by FACS in 3H9⁺ *Tlr9^{-/-}* MRL.*Fas^{lpr}* mice (Fig. 3D). TLR9-deficient 3H9⁺ MRL.*Fas^{lpr}* also had reduced cell-surface expression of CD44 (Fig. 3E) and CD86 (Fig. 3F) compared to TLR9-intact animals within the λ 1⁺ compartment, while the non-autoreactive λ x⁺ compartment in the same animals showed no TLR9-dependent differences for these markers of B cell activation. Thus, TLR9 was required for the activation specifically of the anti-DNA reactive B cell population to progress to AFCs in autoimmune-prone mice.

To characterize the nature of the TLR9-dependent anti-DNA response, we performed immunofluorescence microscopy of spleen sections taken from 19-week old 3H9⁺ *Tlr9^{+/+}* or *Tlr9^{-/-}* MRL.*Fas^{lpr}* mice (Fig. 3G, H). *Tlr9^{+/+}* mice had numerous clusters of λ 1-bright EF

plasmablasts, which were strikingly absent in mice lacking TLR9. In contrast, there were few long-lived $\lambda 1^+$ BM AFCs in either genotype (Supplemental Fig. 2D). EF plasmablasts were peanut agglutinin (PNA)-negative (Supplemental Fig. 2A and 2C), though $\lambda 1^-$ PNA⁺ germinal centers (GCs) were found in both TLR9-deficient and TLR9-sufficient Tg animals (Supplemental Fig. 2A and 2B). These data demonstrate that the activation of anti-DNA B cells, like activation of RF B cells (30), occurs predominantly via the EF pathway.

Autoreactive B cells accumulate in the follicle in *Tlr9*-deficient mice

The absence of spontaneous anti-DNA AFCs in TLR9-deficient animals could have been due to differences in precursor population frequency and/or establishment and maintenance of energy. Since we observed no differences in the primary repertoire or development of anti-DNA $\lambda 1^+$ B cells in the BM (Fig. 2), we next enumerated $\lambda 1^+$ B cells in the spleens and LNs of 3H9⁺ *Tlr9*^{+/+} or 3H9⁺ *Tlr9*^{-/-} MRL.*Fas*^{lpr} as well as 3H9⁻ mice by FACS. Surprisingly, not only were $\lambda 1^+$ anti-DNA cells present in the spleens of TLR9-deficient mice, but the percentage of FO and LN B cells that were $\lambda 1^+$ was actually *greater* in 3H9⁺ *Tlr9*^{-/-} mice than in 3H9⁺ *Tlr9*^{+/+} mice (Fig. 4A and 4D). In contrast, the percentage of marginal zone (MZ) B cells using $\lambda 1$ was unaffected by TLR9 expression (Fig. 4B). The frequencies of non-autoreactive λx^+ B cells in the LN and splenic FO, MZ, or transitional populations were not different in the presence or absence of TLR9 (Supplemental Fig. 3). Importantly, the proportion of CD93⁺ transitional B cells that were $\lambda 1^+$ was also not affected by *Tlr9* genotype (Fig. 4C), indicating that TLR9 does not affect DNA-reactive B cell accumulation prior to completion of maturation. This conclusion is also consistent with the lack of effect of TLR9 expression on $\lambda 1$ or λx usage in Fr. E in the BM and the increased frequency of $\lambda 1$ cells in BM Fr. F (Fig. 2C, 2D). Thus, TLR9 deficiency led to the accumulation of a population of FO anti-DNA B cells, which nonetheless do not progress to AFCs.

Autoreactive B cells in *Tlr9*-deficient mice are Ag-exposed and functionally anergic

We next asked whether TLR9-deficient and TLR9-sufficient anti-DNA B cells were similarly anergic. We first compared surface IgA expression as a function of *Tlr9* genotype in 3H9 Tg MRL.*Fas*^{lpr} mice. Similar to anergic B cells in several models including 3H9 (29, 31, 32), BCR downregulation was observed in both TLR9-deficient and sufficient $\lambda 1^+$ splenic follicular (FO) B cells (Fig. 5A-C). 3H9/V $\lambda 1$ BCR expression was slightly lower in TLR9-deficient compared to TLR9-intact animals (Fig. 5C). In contrast, the nonautoreactive 3H9/V λx BCRs in the same animals were not downregulated compared to non-Tg mice, either with or without *Tlr9* (Fig. 5D-F).

While BCR downregulation indicated Ag exposure, this observation alone did not establish functional anergy. Anergic B cells have high basal BCR signaling but poor responses to *in vitro* IgM crosslinking (2). Therefore, we asked whether TLR9 influenced BCR signaling. Basal Syk phosphorylation was indeed increased in the autoreactive 3H9/V $\lambda 1$ B cell population compared to non-Tg MRL.*Fas*^{lpr}, but this increase did not depend upon *Tlr9* genotype, suggesting that the autoreactive population is anergized with or without TLR9 (Fig. 5G-H). Importantly, there were no differences in basal Syk phosphorylation in the V λx nonautoreactive population with or without either the 3H9 Tg or *Tlr9* (Fig. 5I). In addition, FO B cells from both 3H9⁺ and 3H9⁺ *Tlr9*^{-/-} MRL.*Fas*^{lpr} had similarly high basal intracellular Ca⁺² concentrations compared to Tg-negative animals, which did not increase as much in 3H9⁺ cells compared to non-Tg cells following IgM crosslinking, irrespective of *Tlr9* genotype (Fig. 5J-O). Thus, with respect to both BCR downregulation and signaling, anti-DNA B cells in 3H9 *Tlr9*^{-/-} MRL.*Fas*^{lpr} mice are anergized to a similar extent as their TLR9-intact counterparts.

Anergic B cells have a short half-life, though the reasons for this are unclear (2, 33, 34). The increased number of $\lambda 1^+$ FO B cells in $3H9^+ Tlr9^{-/-}$ MRL.*Fas*^{lpr} versus $3H9^+ Tlr9^{+/+}$ MRL.*Fas*^{lpr} (Fig. 4A) suggested that TLR9 might regulate the survival of anergic anti-DNA B cells. We therefore measured the kinetics of BrdU uptake in $3H9/V\lambda 1^+$ cells from TLR9-intact or -deficient MRL.*Fas*^{lpr} mice. Provided that cells are not proliferating within a particular compartment itself, the frequency of BrdU⁺ B cells in peripheral compartments following long-term labeling is proportional to the rate of entry of cells into that population from the bone marrow as the unlabeled cells resident in that population turn over, as specifically shown for the B cell lineage (35). BrdU was provided by *i.p.* injection twice daily for two or four days. Under these conditions, transitional B cells were labeled with BrdU at a similar rate regardless of *Tlr9* genotype, with approximately half of the $3H9/V\lambda 1$ (Fig. 6A) or $3H9/V\lambda 1^-$ (Fig. 6D) transitional B cells in the spleen having incorporated BrdU by 4 days of labeling, suggesting that rates of immature B cell entry into the spleen from the BM are unaffected by TLR9. In contrast, the frequency of BrdU⁺ cells among $3H9/V\lambda 1^+$ FO B cells was more than 2-fold greater in TLR9-intact MRL.*Fas*^{lpr} compared to *Tlr9*^{-/-} animals (Fig. 6B), consistent with a greater turnover rate of FO B cells in the TLR9-intact animals. This TLR9-dependent difference in labeling kinetics was also observed for $\lambda 1^+$ B cells in the LNs (Fig. 6C). Labeling of the $\lambda 1^-$ FO B cells was also greater in TLR9-sufficient mice (although to a lesser extent than among the $\lambda 1^+$ population, Fig. 6E), most likely reflecting the mixture of both anergic anti-DNA B cells and nonautoreactive edited B cells in the κ^+ population (22). Finally, labeling of LN $\lambda 1^-$ cells was not significantly affected by TLR9 (Fig. 6F).

The TLR9-dependent difference in the rate of BrdU incorporation among $3H9/V\lambda 1$ FO B cells (Fig. 6B) suggested that this population was turning over more rapidly in TLR9-intact than TLR9-deficient $3H9^+$ MRL.*Fas*^{lpr} mice. Alternatively, the difference could have reflected proliferation of TLR9-stimulated activated B cells directly within the compartment. To address this possibility, we measured BrdU incorporation among CD19⁺ CD22⁺ CD44^{low} naive B cells and found a TLR9-dependent difference in label in the $\lambda 1^+$ population (Supplemental Fig. 4A) but not among total naive B cells (Supplemental Fig. 4B). To further evaluate whether TLR9 affected proliferation of FO B cells directly, we pulsed $3H9^+$ MRL.*Fas*^{lpr} mice with BrdU for 2 hr via a single *i.p.* injection; given the short half-life of BrdU, this labels only those cells in S phase at the time of injection. Under these conditions, approximately 10% of B220⁺ BM cells were labeled with BrdU (Supplemental Fig. 4C) but BrdU incorporation in the $\lambda 1^+$ FO population was not significantly above background (Supplemental Fig. 4D-F), suggesting that the vast majority of FO B cells are indeed nonproliferative. In particular, the implied rates of proliferation of FO B cells are much too low to account for proliferation causing the extent of labeling seen over a 2 or 4 day period; rather such labeling must have come from maturation over that time period of a more immature proliferating precursor, as originally proposed by Allman and colleagues (35). Taken together, these results suggest that follicular $3H9/V\lambda 1$ cells are turning over more rapidly in TLR9-intact than -deficient MRL.*Fas*^{lpr} animals, consistent with and resulting in the observed increase in this population's frequency when TLR9 is absent (Fig. 4A).

Tlr9 influences distribution of anti-DNA B cells in the follicle

Previous studies demonstrated that anergic cells, including $3H9/V\lambda 1$ B cells, are excluded from the FO and accumulate at or near the T/B border (33, 36). In *Fas*-deficient animals, $3H9/V\lambda 1$ cells were shown to enter the FO to a much greater extent than in *Fas*-sufficient animals (37). Nonetheless, we noted that in a significant fraction of pre-autoimmune $3H9^+$ MRL.*Fas*^{lpr} follicles the distribution of $\lambda 1^+$ cells did not appear to be as uniform throughout the follicle as was observed in nontransgenic animals (Fig. 7B, 7C). We therefore developed an image analysis algorithm to assess the distribution of $\lambda 1^+$ cells in the FO more rigorously

than can be accomplished by visual inspection of representative images. Using CellProfiler image analysis software, we identified a portion of the B cell follicle that was immediately adjacent to the T cell zone and enumerated the $\lambda 1^+$ pixels in that region. This number was expressed as a ratio to the number of $\lambda 1^+$ pixels in the follicle as a whole, and normalized to the relative areas of the two regions, to define a “distribution index.” A distribution index of 1 would therefore indicate that, per unit area, there are as many $\lambda 1^+$ cells on the edge of the FO closest to the T zone as there are in the FO as a whole, while a distribution index of greater than 1 indicates a relative enrichment of $\lambda 1^+$ cells on the edge of the FO nearest the T zone.

Using this approach, we found that the follicles of nontransgenic MRL.*Fas^{pr}* mice had a median distribution index of 0.93 for $\lambda 1^+$ cells (mean \pm SEM: 0.919 \pm 0.020). In contrast, the median distribution index of 3H9⁺ MRL.*Fas^{pr}* follicles was 1.27 (mean \pm SEM: 1.309 \pm 0.030), indicating a relative enrichment of 3H9/ $\lambda 1$ cells on the T-proximal edge of the FO compared to the FO as a whole (Fig. 7A). The distribution of 3H9/ $\lambda 1$ anti-DNA cells was modestly but significantly lower in the 3H9⁺ *Tlr9*^{-/-} MRL.*Fas^{pr}* group, with a median distribution index of 1.185 (mean \pm SEM: 1.223 \pm 0.032, $p < 0.05$, Fig. 7A, 7D). Thus, *Tlr9* contributes in part to the exclusion of anergic B cells from the follicle and their accumulation at the T/B border.

Discussion

The involvement of TLR9 in SLE has been evident from a number of *in vivo* and *in vitro* experimental systems, but its precise roles remain puzzling and apparently paradoxical. In particular, although TLR9 is required for anti-DNA antibody generation in lupus-prone mice, its *absence* promotes disease in at least five different murine lupus models (6-10). Why is this?

Here we have provided several significant pieces to the puzzle of TLR9 function in systemic autoimmunity. We showed first, using mixed BM chimeras, that TLR9 must be expressed in the B cell compartment for the generation of anti-DNA in the MRL.*Fas^{pr}* model of SLE. Thus, although TLR9 is expressed in many myeloid cells and is linked to the secretion of type I interferons and immune cell activation that may also promote autoAbs, its expression in B cells *per se* is absolutely required for anti-DNA production. We then used the 3H9 BCR Tg model to track the effects of TLR9 expression on the fate of a defined population of autoreactive anti-DNA B cells through development in comparison to non-autoreactive B cells within the same animals. We found that anti-DNA AFCs are produced via an EF plasmablast response rather than a GC, in an entirely TLR9-dependent manner, analogous to the situation for RF B cells (30).

Most unexpectedly, we found that TLR9 also governed peripheral anti-DNA B cell homeostasis, promoting tolerance rather than autoreactivity. In contrast, TLR9 deficiency had no detectable effect on the development, accumulation, labeling kinetics, or receptor editing of anti-DNA B cells in the BM or among immature splenic B cells; nor did TLR9 affect BCR-proximal establishment of anergy. Taken together, these results provide a comprehensive analysis of TLR9's influence on anti-DNA B cells throughout B cell development and maturation, revealing novel and seemingly paradoxical roles for TLR9 in the establishment and maintenance of B cell tolerance.

TLR9 deficiency uncovered a previously unsuspected tolerogenic role of TLR9 in the peripheral B cell compartment: there was a striking accumulation of anergic anti-DNA B cells within the FO and in the LN. Interestingly, this increase was not seen in CD93⁺ immature B cell compartments (“Fraction E”) in either the BM or spleen. Thus, the effects

of TLR9 in preventing autoreactive cell accumulation occur either at the E to F transition or take place within fraction F. This is an important distinction to make because it may relate to the observation that polyreactive B cells in human patients lacking either IRAK-4, MyD88, or Unc93b were not filtered from the repertoire (14). Curiously, elimination of cells reacting in a HEP2-extract ELISA assay, which may relate more directly to the anti-DNA specificity we studied, was only faulty in the IRAK-4 and MyD88-deficient patients but not in patients deficient in UNC93b, a discrepancy that has not yet been resolved. Regardless, the explanation for how the lack of these genes in humans affects autoreactivity in the B cell repertoire—whether negative selection, positive selection, or receptor editing—could not be addressed in human studies. However, based on differences seen in “new emigrant” circulating B cells, these genes were thought to affect the repertoire in the immature rather than mature compartments. In contrast, we found the effects of TLR9 were instead seen on accumulation and turnover rate of mature FO B cells in the periphery; whereas, in developing anti-DNA B cells neither receptor editing nor cellular homeostasis of immature B cells were affected.

There are a number of possible reasons for the apparent differences in our findings and those of Isnardi *et al.* First, the specificities under study were different. In the human studies polyclonal and HEP-2 reactivity were measured, which comprise multiple specificities that may differ in TLR dependence. In this report we focused on a single, well-defined, chromatin-reactive clonotype, allowing for a more precise interpretation of the relationship between BCR specificity and cell fate. Second, though both mice and humans express functional TLR9 during B cell development, there could still be species-specific differences, with mice potentially filtering their B cell compartment at a later stage but in an analogous way. Third, we looked specifically at TLR9 whereas the human studies used less targeted deficiencies based on the availability of patients with rare mutations. These mutations affect multiple signaling pathways that include, but are not limited to, TLR9. Finally, humans lacking these signaling pathways in all cells from birth are immunodeficient, and an indirect effect of this contributing to the different phenotype cannot be excluded.

The expression of TLR9 leads to more rapid turnover in the FO compartment, which in turn leads to a smaller autoreactive compartment at steady state. This tolerogenic role for TLR9 in regulating autoreactive cell lifespan is most likely B cell intrinsic rather than an indirect effect of differences in production of survival factors such as BAFF by non-B cells. This notion is supported by the difference in labeling between the $\text{V}\lambda 1^+$ cells, which are uniformly anti-DNA, and the $\lambda 1^-$ population, which includes both edited non-reactive and anti-DNA cells. In contrast, a B cell-extrinsic effect should have affected all types of B cell. While TLR9 did not affect expression of CD44 or CD86 in non-autoreactive cells, it supported the expression of these markers in DNA-reactive B cells, further illustrating how TLR9 plays an ongoing role in shaping the peripheral self-reactive B cell repertoire.

In concert with the effects of TLR9 on anti-DNA B cell turnover and cell surface marker expression in the mature compartment, TLR9 expression also modestly affected the positioning of these self-reactive B cells. In TLR9-sufficient mice anti-DNA B cells tended to be located closer to the T/B border in contrast to a somewhat less asymmetric FO distribution in TLR9-deficient mice. Localization to the T/B border has been shown in some models of autoreactivity to be linked to *Fas*-independent cell death (38) and so localization might contribute in part to the differences we observed in B cell turnover between TLR9-intact and TLR9-deficient mice.

Despite differences in activation, differentiation and other cell intrinsic effects mediated by TLR9 expression, anergy *per se* (defined as high basal BCR-proximal signaling and poor induced BCR responses) was not affected. Rather, these properties seemed to be directly

controlled by the BCR only. Notably, however, other phenotypes frequently *associated* with anergy, including modulated expression of the BCR and the coactivation marker CD86, as well as a diminished lifespan, were indeed *Tlr9*-dependent. While anergy has been linked to both reduced half-life and altered localization in some studies (34), anergy in HEL/anti-HEL Tg mice has also been dissociated from at least FO exclusion (33, 38). Although definitions of anergy therefore vary significantly from model to model, we define here key aspects of the anti-DNA anergic phenotype that are TLR9-dependent and others that are TLR9-independent. In particular, our data suggest that TLR9 has direct effects on B cell survival and location that cannot be explained by BCR signaling alone. These findings thus demonstrate that anergy, like activation, is fundamentally different for autoreactive B cells specific for self-Ags containing TLR ligands, and explain discrepancies between phenotypes of anti-HEL and anti-DNA anergic B cells (29, 32-34, 38).

An interesting implication of our findings is that all anergic anti-DNA B cells are influenced by TLR9 signals, yet these signals mainly modulate anergy and only occasionally lead to activation. This raises the question of why TLR9 signals are not activating in anergic B cells. B cell anergy induces constitutive SHIP-1 activity (39) which may suppress some—but not all—outcomes of TLR9 signaling as SHIP-1 negatively regulates *in vitro* responses to CpG (40). Nonetheless, this raises the question of how some anergic autoreactive cells do become activated. One possibility is that in rare cells, more extensive BCR crosslinking occurs that overrides anergy, switching the outcome of TLR9 signals from tolerogenic to activating, perhaps by abrogating SHIP-1 activity or other biochemical features of anergy. Alternatively or in addition, further extrinsic signals could alter the outcome of TLR9 signaling in anti-DNA B cells, including T cell-derived signals (41). In any case, the idea of rare activation of otherwise tolerized or clonally ignorant cells is consistent with the oligoclonal nature of the autoantibody response in lupus-prone mice (42) or in people (43).

TLR9 is expressed in the B cells of healthy individuals and animals, and so its tolerogenic functions in limiting anti-DNA cell lifespan must *a priori* be dominant under most circumstances. The striking implication of our results is that, as long as anergy is maintained, TLR9 signaling serves in fact to reduce the autoreactive cell contribution to the repertoire. In this way TLR9 provides an important “regulatory” function. These new insights provide a link in understanding the interplay between TLRs and BCRs in establishing self-tolerance and how this breaks down in autoimmunity.

Supplementary Material

Refer to Web version on PubMed Central for supplementary material.

Acknowledgments

We thank Martin Weigert (University of Chicago, Chicago, IL) for providing 3H9 MRL.*Fas*^{lpr} mice and Dr. Pierre-Andre Cazenave for producing and making available the 10C5 anti- λ x hybridoma, provided to us via Marko Radic (University of Tennessee, Memphis, TN). We thank Eric Meffre and Ann Rothstein for critical reading of the manuscript.

2 Abbreviations used in this paper

AFC	antibody forming cell
ANA	antinuclear antibody
BM	bone marrow
EF	extrafollicular

EMA	ethidium monoazide bromide
FO	follicle / follicular
GC	germinal center
LN	lymph node
MZ	marginal zone
PNA	peanut agglutinin
RF	rheumatoid factor
RS	recombination sequence
SLE	systemic lupus erythematosus
Tg	transgene / transgenic

References

1. Wardemann H, Yurasov S, Schaefer A, Young JW, Meffre E, Nussenzweig MC. Predominant autoantibody production by early human B cell precursors. *Science*. 2003; 301:1374–1377. [PubMed: 12920303]
2. Cambier JC, Gauld SB, Merrell KT, Vilen BJ. B-cell anergy: from transgenic models to naturally occurring anergic B cells? *Nat Rev Immunol*. 2007; 7:633–643. [PubMed: 17641666]
3. Luning Prak ET, Monestier M, Eisenberg RA. B cell receptor editing in tolerance and autoimmunity. *Annals of the New York Academy of Sciences*. 2011; 1217:96–121. [PubMed: 21251012]
4. Barbalat R, Ewald SE, Mouchess ML, Barton GM. Nucleic acid recognition by the innate immune system. *Annu. Rev. Immunol*. 2011; 29:185–214. [PubMed: 21219183]
5. Christensen SR, Shupe J, Nickerson K, Kashgarian M, Flavell RA, Shlomchik MJ. Toll-like receptor 7 and TLR9 dictate autoantibody specificity and have opposing inflammatory and regulatory roles in a murine model of lupus. *Immunity*. 2006; 25:417–428. [PubMed: 16973389]
6. Nickerson KM, Christensen SR, Shupe J, Kashgarian M, Kim D, Elkon K, Shlomchik MJ. TLR9 Regulates TLR7- and MyD88-Dependent Autoantibody Production and Disease in a Murine Model of Lupus. *J Immunol*. 2010; 184:1840–1848. [PubMed: 20089701]
7. Lartigue A, Courville P, Auquit I, François A, Arnoult C, Tron F, Gilbert D, Musette P. Role of TLR9 in anti-nucleosome and anti-DNA antibody production in lpr mutation-induced murine lupus. *J Immunol*. 2006; 177:1349–1354. [PubMed: 16818796]
8. Santiago-Raber M-L, Dunand-Sauthier I, Wu T, Li Q-Z, Uematsu S, Akira S, Reith W, Mohan C, Kotzin BL, Izui S. Critical role of TLR7 in the acceleration of systemic lupus erythematosus in TLR9-deficient mice. *J Autoimmun*. 2009
9. Stoehr AD, Schoen CT, Mertes MMM, Eiglmeier S, Holeccka V, Lorenz AK, Schommartz T, Schoen A-L, Hess C, Winkler A, Wardemann H, Ehlers M. TLR9 in Peritoneal B-1b Cells Is Essential for Production of Protective Self-Reactive IgM To Control Th17 Cells and Severe Autoimmunity. *J Immunol*. 2011
10. Yu P, Wellmann U, Kunder S, Quintanilla-Martinez L, Jennen L, Dear N, Amann K, Bauer S, Winkler TH, Wagner H. Toll-like receptor 9-independent aggravation of glomerulonephritis in a novel model of SLE. *Int Immunol*. 2006; 18:1211–1219. [PubMed: 16798839]
11. Christensen SR, Shlomchik MJ. Regulation of lupus-related autoantibody production and clinical disease by Toll-like receptors. *Seminars in Immunology*. 2007; 19:11–23. [PubMed: 17276080]
12. Fields ML, Metzgar MH, Hondowicz BD, Kang S-A, Alexander ST, Hazard KD, Hsu AC, Du Y-Z, Prak EL, Monestier M, Erikson J. Exogenous and endogenous TLR ligands activate anti-chromatin and polyreactive B cells. *J Immunol*. 2006; 176:6491–6502. [PubMed: 16709806]
13. Azulay-Debby H, Edry E, Melamed D. CpG DNA stimulates autoreactive immature B cells in the bone marrow. *Eur J Immunol*. 2007; 37:1463–1475. [PubMed: 17474151]

14. Isnardi I, Ng Y-S, Srdanovic I, Motaghedi R, Rudchenko S, von Bernuth H, Zhang S-Y, Puel A, Jouanguy E, Picard C, Garty B-Z, Camcioglu Y, Doffinger R, Kumararatne D, Davies G, Gallin JI, Haraguchi S, Day NK, Casanova J-L, Meffre E. IRAK-4- and MyD88-dependent pathways are essential for the removal of developing autoreactive B cells in humans. *Immunity*. 2008; 29:746–757. [PubMed: 19006693]
15. Erikson J, Radic MZ, Camper SA, Hardy RR, Carmack C, Weigert M. Expression of anti-DNA immunoglobulin transgenes in non-autoimmune mice. *Nature*. 1991; 349:331–334. [PubMed: 1898987]
16. Roark JH, Kuntz CL, Nguyen KA, Caton AJ, Erikson J. Breakdown of B cell tolerance in a mouse model of systemic lupus erythematosus. *J Exp Med*. 1995; 181:1157–1167. [PubMed: 7532679]
17. Radic MZ, Mackle J, Erikson J, Mol C, Anderson WF, Weigert M. Residues that mediate DNA binding of autoimmune antibodies. *J Immunol*. 1993; 150:4966–4977. [PubMed: 8496598]
18. Ibrahim SM, Weigert M, Basu C, Erikson J, Radic MZ. Light chain contribution to specificity in anti-DNA antibodies. *J Immunol*. 1995; 155:3223–3233. [PubMed: 7673735]
19. Li Y, Louzoun Y, Weigert M. Editing anti-DNA B cells by V λ mbdax. *J Exp Med*. 2004; 199:337–346. [PubMed: 14757741]
20. Chen C, Nagy Z, Radic MZ, Hardy RR, Huszar D, Camper SA, Weigert M. The site and stage of anti-DNA B-cell deletion. *Nature*. 1995; 373:252–255. [PubMed: 7816141]
21. Chen C, Radic MZ, Erikson J, Camper SA, Litwin S, Hardy RR, Weigert M. Deletion and editing of B cells that express antibodies to DNA. *J Immunol*. 1994; 152:1970–1982. [PubMed: 8120401]
22. Gay D, Saunders T, Camper S, Weigert M. Receptor editing: an approach by autoreactive B cells to escape tolerance. *J Exp Med*. 1993; 177:999–1008. [PubMed: 8459227]
23. Shlomchik MJ, Aucoin AH, Pisetsky DS, Weigert MG. Structure and function of anti-DNA autoantibodies derived from a single autoimmune mouse. *Proc Natl Acad Sci USA*. 1987; 84:9150–9154. [PubMed: 3480535]
24. Losman MJ, Fasy TM, Novick KE, Monestier M. Monoclonal autoantibodies to subnucleosomes from a MRL/Mp(-)/+ mouse. Oligoclonality of the antibody response and recognition of a determinant composed of histones H2A, H2B, and DNA. *J Immunol*. 1992; 148:1561–1569. [PubMed: 1371530]
25. Hannum LG, Ni D, Haberman AM, Weigert MG, Shlomchik MJ. A disease-related rheumatoid factor autoantibody is not tolerized in a normal mouse: implications for the origins of autoantibodies in autoimmune disease. *J Exp Med*. 1996; 184:1269–1278. [PubMed: 8879198]
26. Meng W, Li Y, Xue E, Satoh M, Peck AB, Cohen PL, Eisenberg RA, Prak E. T. Luning. B-Cell Tolerance Defects in the B6.Aec1/2 Mouse Model of Sjogren's Syndrome. *Journal of clinical immunology*. 2012
27. Carpenter AE, Jones TR, Lamprecht MR, Clarke C, Kang IH, Friman O, Guertin DA, Chang JH, Lindquist RA, Moffat J, Golland P, Sabatini DM. CellProfiler: image analysis software for identifying and quantifying cell phenotypes. *Genome Biol*. 2006; 7:R100. [PubMed: 17076895]
28. Panigrahi AK, Goodman NG, Eisenberg RA, Rickels MR, Naji A, Prak E. T. Luning. RS rearrangement frequency as a marker of receptor editing in lupus and type 1 diabetes. *J Exp Med*. 2008; 205:2985–2994. [PubMed: 19075293]
29. Mandik-Nayak L, Seo SJ, Sokol C, Potts KM, Bui A, Erikson J. MRL-lpr/lpr mice exhibit a defect in maintaining developmental arrest and follicular exclusion of anti-double-stranded DNA B cells. *J Exp Med*. 1999; 189:1799–1814. [PubMed: 10359584]
30. Herlands RA, Christensen SR, Sweet RA, Hershberg U, Shlomchik MJ. T cell-independent and toll-like receptor-dependent antigen-driven activation of autoreactive B cells. *Immunity*. 2008; 29:249–260. [PubMed: 18691914]
31. Heltemes-Harris L, Liu X, Manser T. Progressive surface B cell antigen receptor down-regulation accompanies efficient development of antinuclear antigen B cells to mature, follicular phenotype. *J Immunol*. 2004; 172:823–833. [PubMed: 14707052]
32. Rathmell JC, Fournier S, Weintraub BC, Allison JP, Goodnow CC. Repression of B7.2 on self-reactive B cells is essential to prevent proliferation and allow Fas-mediated deletion by CD4(+) T cells. *J Exp Med*. 1998; 188:651–659. [PubMed: 9705947]

33. Cyster JG, Goodnow CC. Antigen-induced exclusion from follicles and anergy are separate and complementary processes that influence peripheral B cell fate. *Immunity*. 1995; 3:691–701. [PubMed: 8777715]
34. Mandik-Nayak L, Seo S. j. Eaton-Bassiri A, Allman D, Hardy RR, Erikson J. Functional consequences of the developmental arrest and follicular exclusion of anti-double-stranded DNA B cells. *J Immunol*. 2000; 164:1161–1168. [PubMed: 10640726]
35. Allman DM, Ferguson SE, Lentz VM, Cancro MP. Peripheral B cell maturation. II. Heat-stable antigen(hi) splenic B cells are an immature developmental intermediate in the production of long-lived marrow-derived B cells. *J Immunol*. 1993; 151:4431–4444. [PubMed: 8409411]
36. Fields ML, Hondowicz BD, Wharton GN, Adair BS, Metzgar MH, Alexander ST, Caton AJ, Erikson J. The regulation and activation of lupus-associated B cells. *Immunol Rev*. 2005; 204:165–183. [PubMed: 15790358]
37. Fields ML, Sokol CL, Eaton-Bassiri A, Seo S, Madaio MP, Erikson J. Fas/Fas ligand deficiency results in altered localization of anti-double-stranded DNA B cells and dendritic cells. *J Immunol*. 2001; 167:2370–2378. [PubMed: 11490027]
38. Ekland EH, Forster R, Lipp M, Cyster JG. Requirements for follicular exclusion and competitive elimination of autoantigen-binding B cells. *J Immunol*. 2004; 172:4700–4708. [PubMed: 15067045]
39. O’Neill SK, Getahun A, Gauld SB, Merrell KT, Tamir I, Smith MJ, Dal Porto JM, Li Q-Z, Cambier JC. Monophosphorylation of CD79a and CD79b ITAM Motifs Initiates a SHIP-1 Phosphatase-Mediated Inhibitory Signaling Cascade Required for B Cell Anergy. *Immunity*. 2011; 35:746–756. [PubMed: 22078222]
40. Gabhann JN, Higgs R, Brennan K, Thomas W, Damen JE, Larbi N. Ben, Krystal G, Jefferies CA. Absence of SHIP-1 Results in Constitutive Phosphorylation of Tank-Binding Kinase 1 and Enhanced TLR3-Dependent IFN- α Production. *J. Immunol*. 2010; 184:2314–2320. [PubMed: 20100929]
41. Seo, S.-j.; Fields, ML.; Buckler, JL.; Reed, AJ.; Mandik-Nayak, L.; Nish, SA.; Noelle, RJ.; Turka, LA.; Finkelman, FD.; Caton, AJ.; Erikson, J. The impact of T helper and T regulatory cells on the regulation of anti-double-stranded DNA B cells. *Immunity*. 2002; 16:535–546. [PubMed: 11970877]
42. Shlomchik M, Mascelli M, Shan H, Radic MZ, Pisetsky D, Marshak-Rothstein A, Weigert M. Anti-DNA antibodies from autoimmune mice arise by clonal expansion and somatic mutation. *J Exp Med*. 1990; 171:265–292. [PubMed: 2104919]
43. Bouvet JP, Wu YX, Pillot J. Restricted heterogeneity of polyclonal rheumatoid factors. *Arthritis and rheumatism*. 1987; 30:998–1005. [PubMed: 3663264]

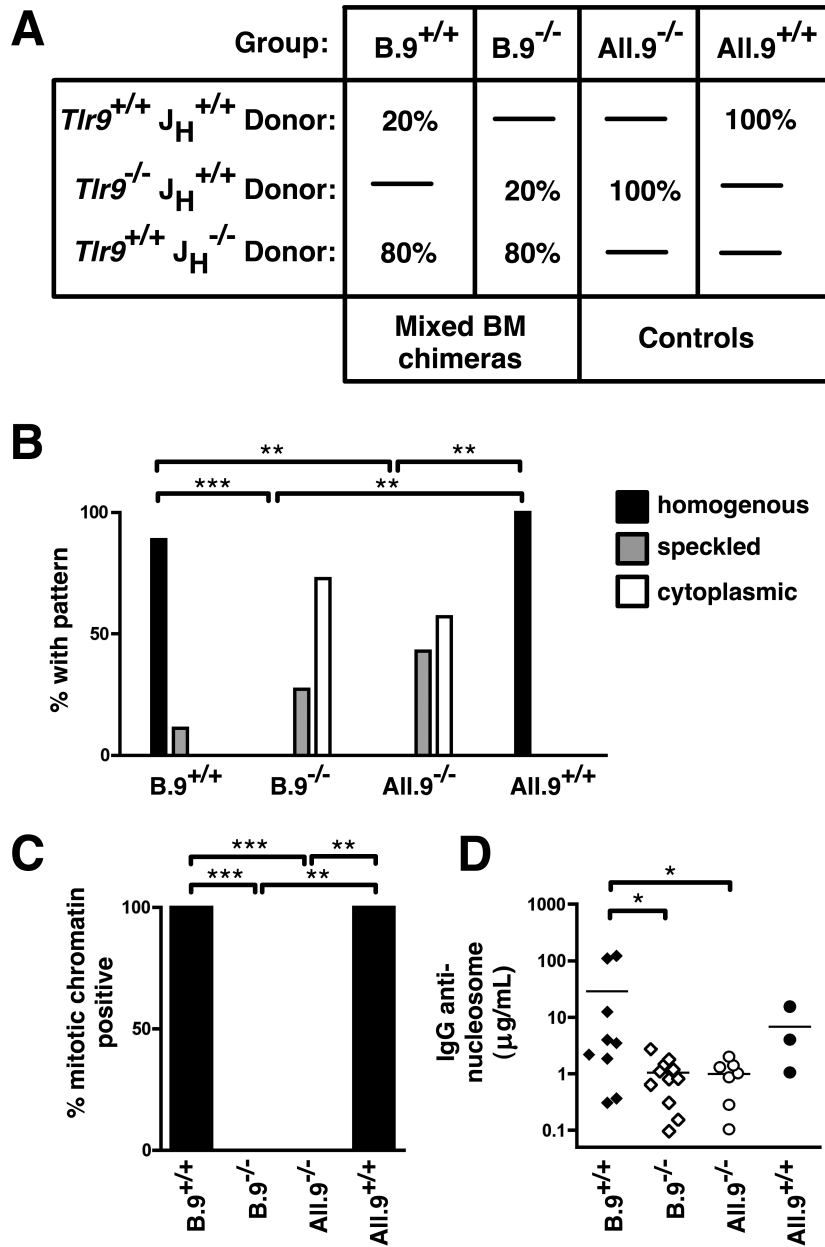


Figure 1. Anti-DNA Ab production requires B-intrinsic TLR9

(A) Scheme to generate MRL.*Fas*^{dpf} mixed chimeras. (B) Sera were assessed by HEP-2 ANA at 16 wks post reconstitution, and the dominant pattern scored. (C) HEP-2 ANA were scored for presence or absence of mitotic chromatin staining. (D) Anti-nucleosome IgG was measured by ELISA. Comparisons in (B) and (C) by two-sided Fisher's exact test. Data are pooled from 5 independent cohorts.

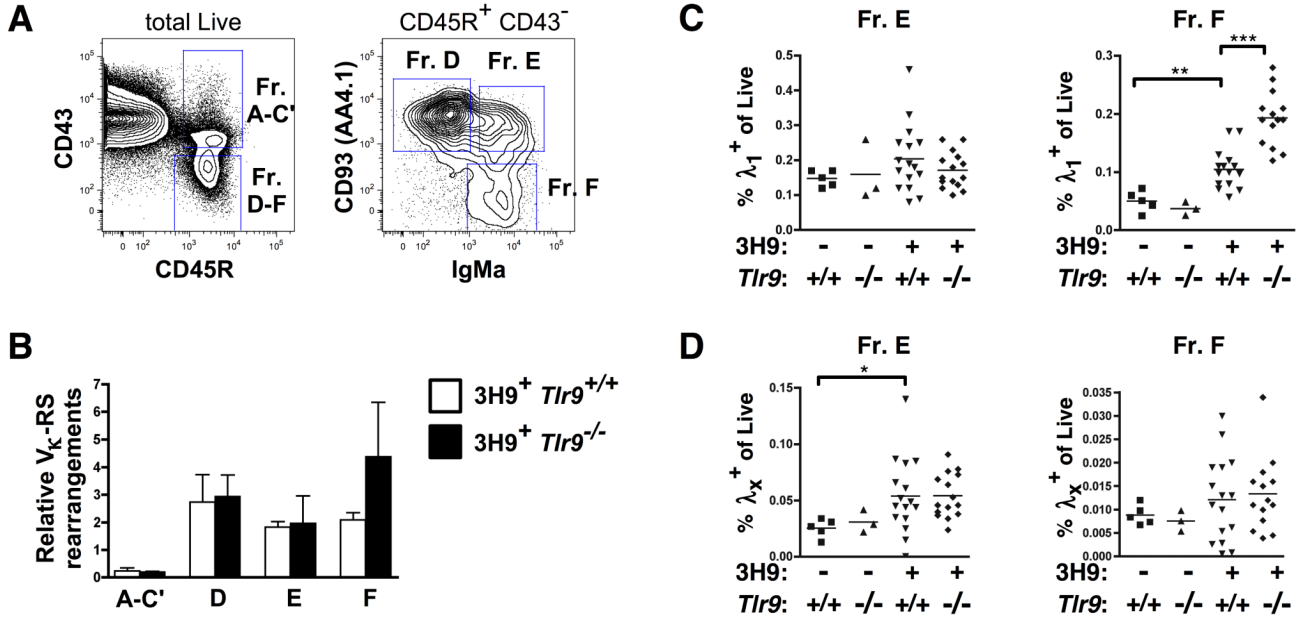


Figure 2. L chain editing is not impaired in TLR9-deficient MRL.Fas^{lpr} mice

(A) Sorting strategy for isolation of BM B cell Hardy fractions in 6-9 wk old mice. Representative staining from a 3H9⁺ Tlr9^{+/+} MRL.Fas^{lpr} animal is shown. (B) qPCR of genomic V_κ-RS rearrangements from fractions sorted in (A), expressed relative to a total B6 splenocyte κ⁺ B cell control. *n*=3 per group from 3 independent sorts of *n*=1 per genotype each. (C) Proportion of live BM cells that are λ₁⁺ B220⁺ CD93⁺ (Fraction E, *left*) or λ₁⁺ B220⁺ CD93⁻ (Fraction F, *right*). (D) Proportion of live BM cells that are λ_x⁺ B220⁺ CD93⁺ (Fraction E, *left*) or λ_x⁺ B220⁺ CD93⁻ (Fraction F, *right*). Data in (C) and (D) pooled from 5 cohorts of 13-20 wk old mice.

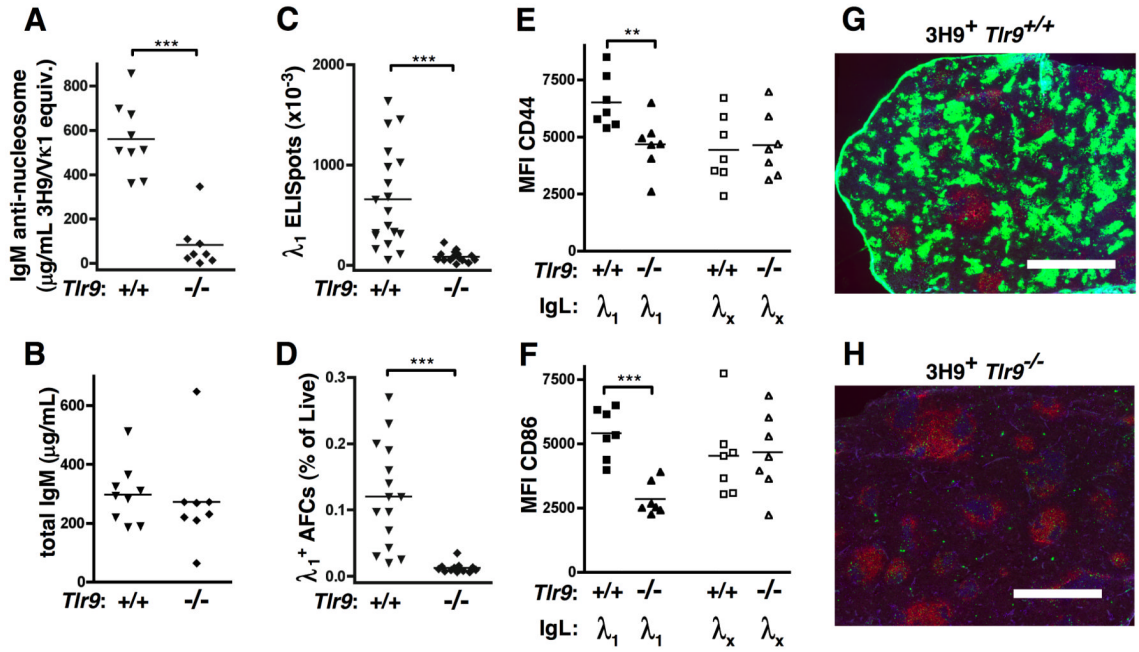


Figure 3. TLR9 is required for anti-DNA antibodies in 3H9 MRL.Fas^{lpr} mice

(A) Serum anti-nucleosome IgM measured by ELISA from 17-20 wk old mice. (B) Total serum IgM measured by ELISA. Data in (A) and (B) pooled from 3 independent cohorts. (C) Splenic AFCs secreting λ₁ IgM Abs detected by ELISPOT. Data are pooled from 5 independent cohorts. (D) TCRβ⁻ CD44⁺ CD138⁺ surface-λ1^{int} intracellular-λ1/2^{high} splenic AFCs enumerated by FACS. Data are pooled from 4 independent cohorts. (E) CD44 and (F) CD86 mean fluorescence intensity (MFI) was measured on CD19⁺ splenocytes. Data in (E) and (F) are representative of 3 independent experiments. (G, H) Immunofluorescent staining of spleen sections from 19 wk old (G) 3H9⁺ Tlr9^{+/+} and (H) 3H9⁺ Tlr9^{-/-} MRL.Fas^{lpr} with CD19 (red), λ1 (green), and CD4 (blue). Scale bar = 1 mm.

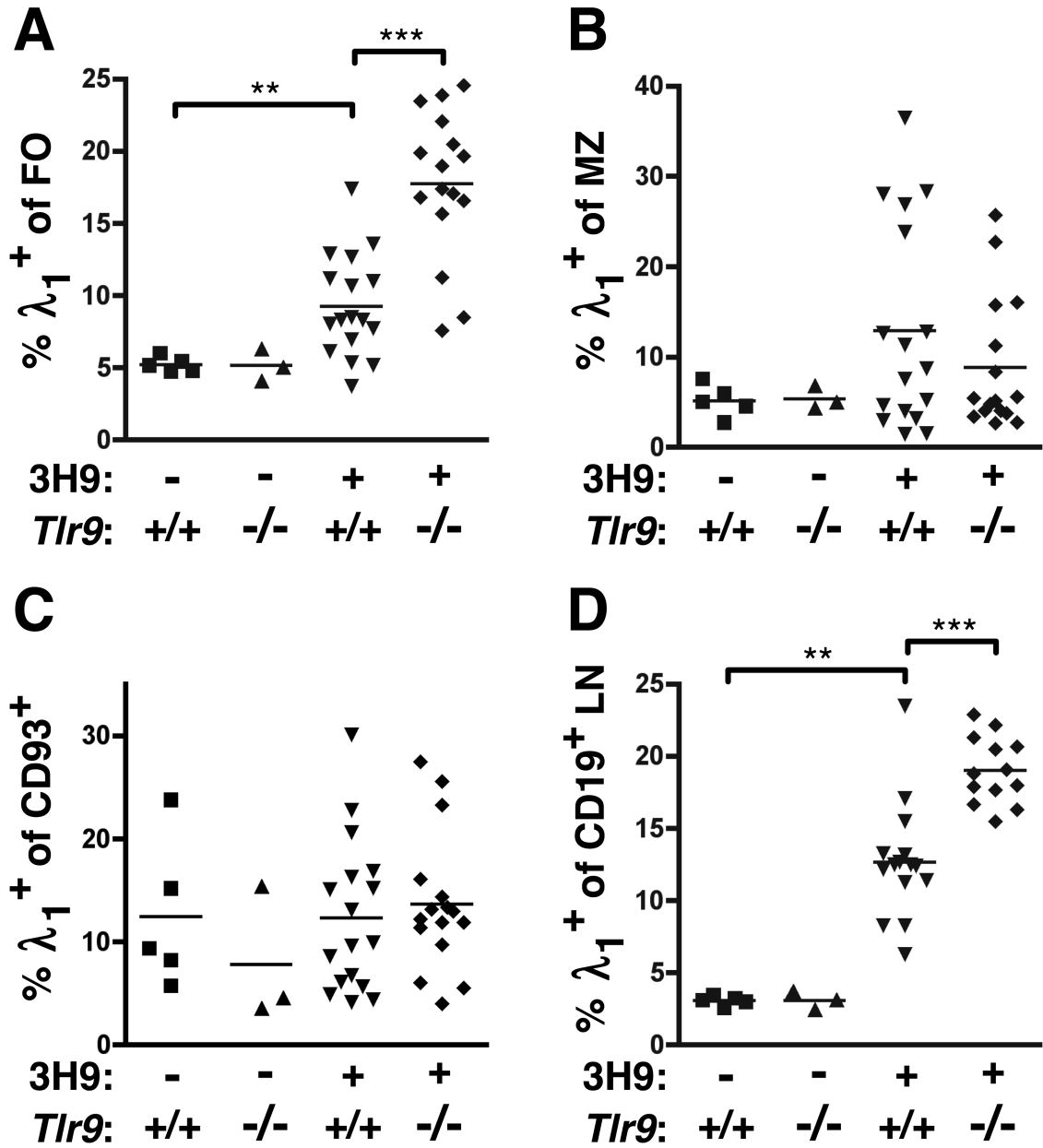


Figure 4. Anti-DNA B cells are expanded in TLR9-deficient mice

Proportion of λ_1^+ cells among (A) CD19⁺ CD93⁻ CD21/35^{int} CD23⁺ FO splenocytes, (B) CD19⁺ CD93⁻ CD21/35⁺ CD23⁻ MZ splenocytes, (C) CD19⁺ CD93⁺ transitional B cells, and (D) CD19⁺ B cells isolated from axillary LNs by FACS. Data are pooled from 5 cohorts of 13-20 wk old mice.

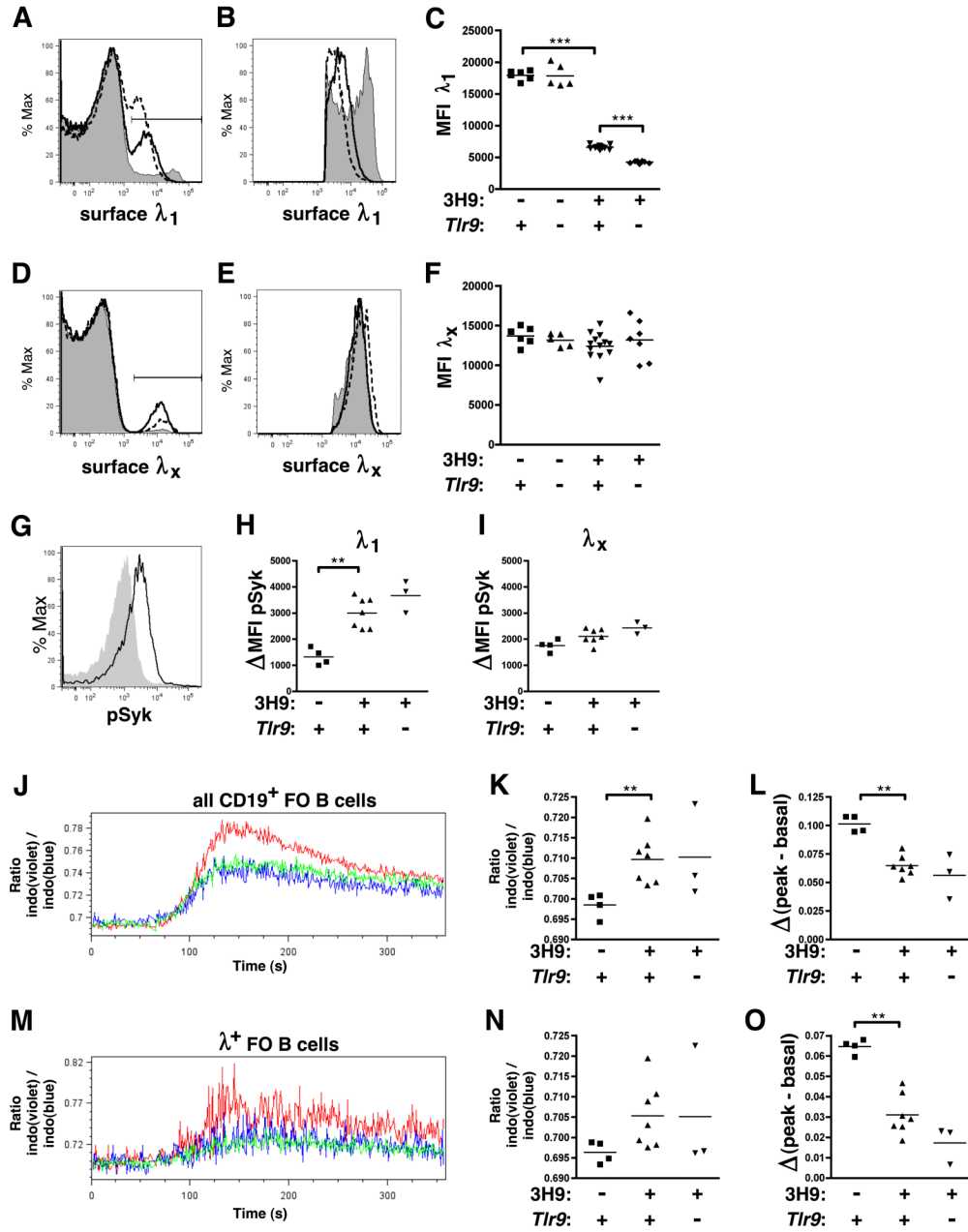


Figure 5. λ_1^+ B cells in TLR9-deficient mice are Ag-experienced and anergic
(A) Representative overlays of surface λ_1 staining among $CD22^+ CD21/35^{int} CD23^+$ splenic FO B cells from 6-8 wk old $3H9^- Tlr9^{+/+}$ MRL.*Fas^{lpr}* (gray shaded), $3H9^+ Tlr9^{+/+}$ MRL.*Fas^{lpr}* (solid line) and $3H9^+ Tlr9^{-/-}$ MRL.*Fas^{lpr}* (dashed line) **(B)** Overlays of surface λ_1^+ staining in (A), gated on the λ_1^+ population. **(C)** MFI of surface λ_1^+ staining among the λ_1^+ population. **(D-F)** Overlays and MFI of surface λ_x staining among FO B cells from the same animals in (A-C). Data are representative of at least 4 (λ_1) or 3 (λ_x) independent experimental cohorts. **(G)** Representative overlay of anti-phosphorylated Syk staining in $CD22^+ \lambda_1^+$ B cells from 8-9 wk old $3H9^-$ MRL.*Fas^{lpr}* mice either fixed immediately upon

spleen disaggregation (*solid line*) or fixed and treated with alkaline phosphatase (*gray shaded*). **(H)** Change in pSyk MFI between untreated or alkaline-phosphatase treated CD22⁺ λ 1⁺ B cells. **(I)** Change in pSyk MFI between untreated or alkaline-phosphatase treated CD22⁺ λ x⁺ B cells. **(J)** Representative overlay of indo-1(violet) / indo-1(blue) ratio over time among CD19⁺ CD35^{int} CD23⁺ FO B cells in 8-9 wk old 3H9⁻ MRL.*Fas^{lpr}* (red), 3H9⁺ *Tlr9^{+/-}* MRL.*Fas^{lpr}* (blue) or 3H9⁺ *Tlr9^{-/-}* MRL.*Fas^{lpr}* (green). Anti-IgM was added at t=60s. **(K)** Basal indo-1(violet) / indo-1(blue) ratio was determined as the mean ratio for t=14s to t=45s. **(L)** Inducible Ca⁺² flux expressed as the difference between peak indo-1(violet) / indo-1(blue) ratio (mean from t=118s to t=159s) and basal indo-1 ratio. **(M-O)** Similar plots to (J-L) with the addition of an anti- λ 1/2 F_(ab) gate. Data are representative of 3 independent experiments, *n*=3-7 per group.

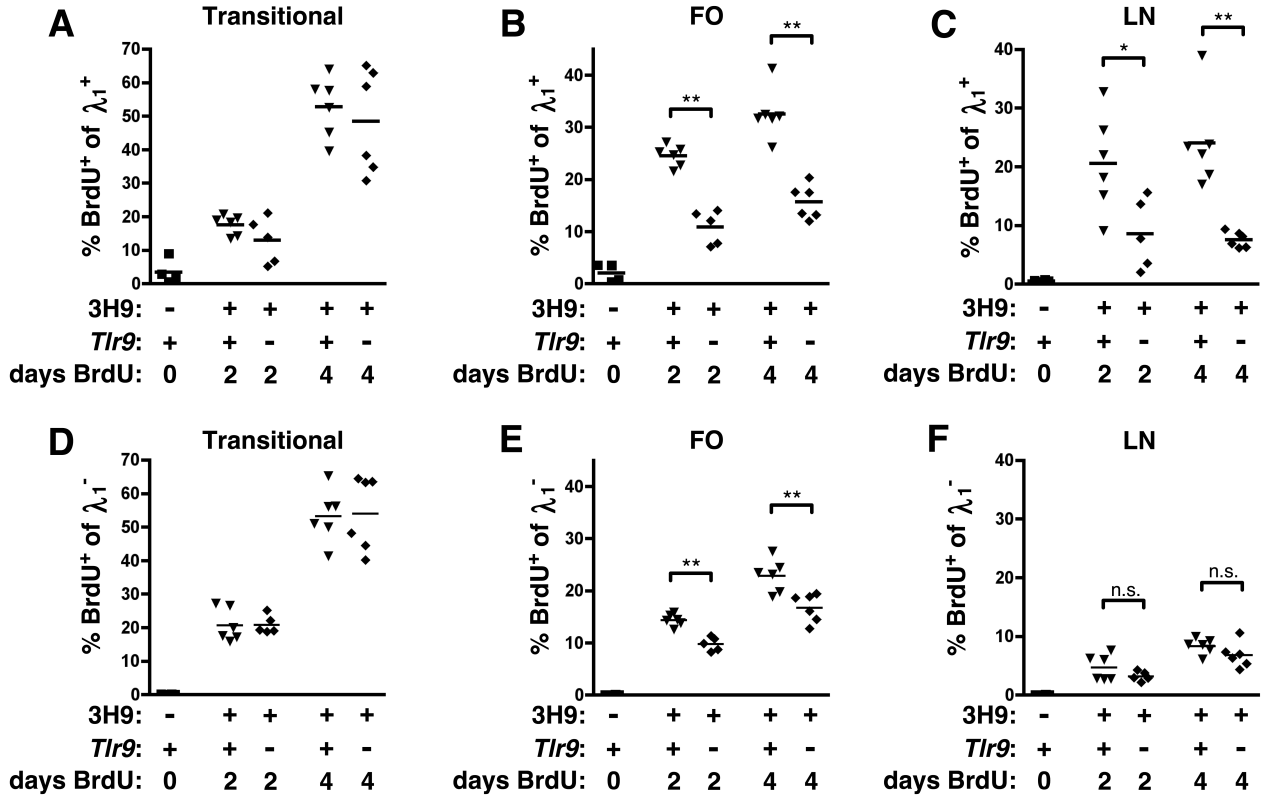


Figure 6. λ_1^+ B cells are longer-lived in TLR9-deficient mice

8-10 wk old mice were given 0.5 mg BrdU *i.p.* every 12 hours for 0, 2 or 4 days before sacrifice. **(A)** Splenic CD22⁺ CD93⁺ λ_1^+ transitional B cells, **(B)** splenic CD22⁺ CD21/35^{int} CD23⁺ λ_1^+ FO B cells, or **(C)** axillary LN CD22⁺ λ_1^+ B cells were evaluated for BrdU incorporation by FACS. **(D-F)** BrdU incorporation in transitional, FO, and LN populations gated on λ_1^- cells. Data are pooled from 4 independent experiments, *n*=4-6 animals per timepoint and genotype.

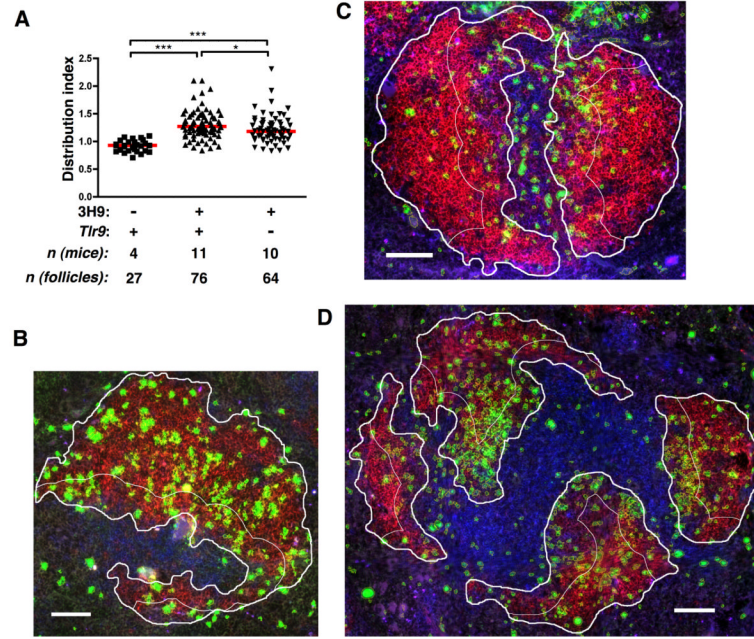


Figure 7. TLR9 controls localization of autoreactive λ_1^+ B cells

(A) Distribution of λ_1^+ B cells in the FO of 6-12 wk old MRL.*Fas^{lpr}* mice of the indicated genotypes. Distribution was determined as described in the text and Methods. Each symbol represents a single follicle. (B-D) Example B cell FO images for (B) nontransgenic MRL.*Fas^{lpr}* (index=0.94), (C) 3H9⁺ *Tlr9^{+/+}* MRL.*Fas^{lpr}* (index=1.56) or (D) 3H9⁺ *Tlr9^{-/-}* MRL.*Fas^{lpr}* (index=1.18), stained with CD19 (red), λ_1 (green) and CD4 (blue). λ_1^+ areas identified by CellProfiler software are outlined in yellow, while the user-defined FO is outlined in thick white lines and the T/B border-proximal region of the FO is outlined in thin white lines. Scale bar = 100 μ m.